Received: 18 February 2026 | Revised: 20 May 2026 | Accepted: 22 June 2026 | Published online: 15 July 2026

RESEARCH ARTICLE

Journal of Optics and Photonics Research
2026, Vol. 00(00) 1–11
DOI: 10.47852/bonviewJOPR62029416

BON VIEW PUBLISHING

# Performance Analysis of a 16-QAM Directly Modulated OFDM Visible Optical Wireless Link Without External Modulators

**Mahmoud Alhalabi**[1,*]

[1] *Department of Electrical and Electronic Engineering, Istanbul Yeni Yuzyil University, Türkiye*

**Abstract:** This paper presents a performance analysis of a directly modulated direct-detection orthogonal frequency division multiplexing-based visible light communication system designed for high-speed and low-complexity transmission. The proposed architecture employs 16-Quadrature Amplitude Modulation (16-QAM) and achieves a data rate of 15 Gbps over a 500 m line-of-sight link while eliminating the need for external optical modulators and transmission-line amplifiers. The system was modeled and evaluated in the OptiSystem environment using a 1024-point fast Fourier transform with 512 active subcarriers, a cyclic prefix, and a directly modulated laser operating at 550 nm. Performance was assessed in terms of bit error rate (BER), optical signal-to-noise ratio (OSNR), error vector magnitude (EVM), maximum Q factor, and received optical power. The results show that the proposed architecture maintains BER $\leq 10^{-3}$ when the OSNR is approximately 32 dB or higher, confirming the feasibility of reliable 16-QAM orthogonal frequency division multiplexing (OFDM) transmission without external amplification. In addition, the analysis demonstrates that beam divergence is a critical design factor, since larger divergence angles reduce received optical power density and degrade both BER and EVM. A comparison between theoretical and simulated received power shows close agreement, validating the adopted link-budget model. The results confirm that the proposed directly modulated OFDM architecture provides an energy-efficient and cost-effective solution for short-to-medium-range high-speed visible optical wireless communication.

**Keywords:** visible light communication, optical wireless communication, OFDM, DM-DD-OFDM-VLC, BER

## 1. Introduction

Since the beginning of the 21st century, the proliferation of interconnected devices has substantially altered daily life, facilitating immediate and widespread information availability and enhancing living standards. Advances in networking and telecommunications have generated novel applications in domains including medical care, intelligent residential systems, and mobility [1, 2]. Nevertheless, this shift introduces considerable obstacles [3]. Increasing congestion of the radio frequency spectrum, alongside heightened awareness of possible health effects, has prompted investigation into complementary wireless methods [4]. Visible light communication (VLC) represents one such notable and emerging alternative. Utilizing white light-emitting diodes (LEDs), VLC enables dual-functionality for both illumination and data transfer [5]. In contrast to radio frequency systems, VLC functions within the 380–750 nm wavelength range, corresponding to frequencies of 430–790 THz. A principal advantage of VLC is its safety for human exposure and its lack of interference with sensitive electronic equipment. Furthermore, it operates within a broad, license-free spectral band, providing a distinct benefit compared to regulated radio frequency alternatives. The technology is also highly energy-efficient, capitalizing on the low power consumption and extended operational life inherent to LED lighting. These attributes collectively position VLC as a sustainable and economical solution aligned with contemporary communication needs [6–10]. A comprehensive overview of intensity modulated and directly detected optical orthogonal frequency division multiplexing (IM/DD-OOFDM) techniques for optical wireless communication (OWC) is provided to tackle path loss issues and alleviate noise reflections [11, 12]. IM/DD-OFDM has been extensively studied for economical optical access, showcasing high spectral efficiency with modulation formats such as 16-Quadrature Amplitude Modulation (16-QAM) [13]. The choice of modulation typically takes into account factors such as computational complexity, spectrum, power efficiency, and resistance to environmental noise challenges [14]. In VLC systems, orthogonal frequency division multiplexing (OFDM) is commonly utilized due to its enhanced spectral efficiency and its robustness against multipath reflections, which aids in minimizing noise from the environment. OFDM is categorized as a multicarrier modulation technique that operates multiple subcarriers simultaneously. This method capitalizes on high spectral and power efficiency, resilience to frequency-selective channels, and the benefit of one-tap equalization. Rather than transmitting a high-rate data stream over a single subcarrier, OFDM makes use of numerous closely spaced orthogonal subcarriers, broadcasting

***Corresponding author:** Mahmoud Alhalabi, Department of Electrical and Electronic Engineering, Istanbul Yeni Yuzyil University, Türkiye. Email: mahmoud.alhalabi@yeniyuzyil.edu.tr

information similarly to traditional single-carrier modulation techniques within comparable bandwidths [15]. Numerous studies have been undertaken regarding VLC modulation leveraging OFDM methods, with different researchers examining this area. Various single-component modulation variants of OFDM have emerged, including Direct Current biased Optical OFDM [16], Asymmetrically Clipped Optical OFDM [17], Pulse Amplitude Modulated Discrete Multitone, Unipolar OFDM, and enhanced U-OFDM [18–23]. Conversely, hybrid OFDM techniques with multi-component modulation involve Asymmetrically Clipped DC-biased Optical OFDM, Hybrid Asymmetrically Clipped Optical OFDM, Asymmetrically Clipped Absolute Value Optical OFDM, and Layered Asymmetrically Clipped DC-biased Optical OFDM [24, 25]. Through the use of OFDM modulation, a real-valued, non-negative signal is generated, conforming to the IM/DD principle, which is critical for VLC technology. In this paper, we introduce a cost-efficient optical OFDM communication system. Our proposed system, referred to as optical directly modulated direct-detection OFDM-based VLC (DM-DD-OFDM-VLC), is developed, assessed, and simulated in the context of VLC technology, offering high data rate transmission, excellent spectral efficiency, and reduced path loss. Unlike traditional optical OFDM systems, our method does not necessitate any optical modulator at the central office, nor any optical or electrical amplifiers in the transmission path.

## 1.1. Related works

Recent literature has extensively explored the optimization of VLC to meet the growing demands of high-speed, localized data transmission. A significant portion of this research has focused on fundamental channel modeling, transceiver design, and overcoming environmental limitations. For instance, several studies have evaluated VLC application potential across diverse environments, ranging from indoor positioning systems utilizing light fingerprinting to vehicular communication networks under varying weather conditions [26–31]. Furthermore, advanced infrastructure concepts, such as the deployment of Optical Reconfigurable Intelligent Surfaces, have been modeled to optimize ray tracing and meet stringent error rate targets [32–35].

To maximize spectral efficiency within these optical links, OFDM has emerged as a dominant modulation strategy. Research into free-space optical (FSO) and VLC channels has highlighted critical trade-offs between computational complexity and power efficiency [36, 37]. Innovations such as constellation predistorters have been introduced to linearize OFDM signals, while robust all-optical OFDM architectures have demonstrated resilience against atmospheric attenuation in outdoor Li-Fi settings [38, 39].

## 1.2. Research gap and proposed contribution

Although OFDM-based visible optical wireless and VLC systems have been widely investigated, much of the recent literature has focused either on improving specific optical OFDM variants or on achieving very high transmission capacity using architectures that involve more complex optical processing and hardware. In parallel, directly modulated optical wireless systems have also been explored as lower-cost alternatives, but the practical trade-off between hardware simplification and achievable multi-gigabit performance in short-to-medium-range visible optical wireless links remains insufficiently discussed in a focused manner.

## 1.3. Paper organization

The remainder of this paper is structured as follows: Section 2 provides the mathematical derivation of the VLC channel model. Section 3 details the proposed system architecture and evaluates the performance through a discussion of simulation results. Finally, Section 4 concludes the paper and summarizes key findings.

## 2. Mathematical Analysis of the DM-DD-OFDM-VLC System

The mathematical formulation of the proposed DM-DD-OFDM-VLC system is developed to describe the complete transmission chain, including optical power propagation over the line-of-sight (LoS) channel, OFDM signal formation in the electrical domain, optical-to-electrical conversion at the receiver, and the subsequent evaluation of error vector magnitude (EVM) and BER under the assumed operating conditions. The DM-DD-OFDM-VLC system utilizes a laser diode as the optical transmitter to establish wireless connectivity with the receiver. In this configuration, free space serves as the primary propagation medium for information transfer. Given that the performance of such systems is highly sensitive to the characteristics of the transmission channel, characterizing the propagation medium is essential. For a LoS configuration, the received optical power, $P_R$, is defined by the following expression:

$$\mathrm{P_R} = \mathrm{P_T}\frac{\mathrm{d_R^2}}{(\mathrm{d_T} + \theta R)^2} 10^{\frac{\mathrm{TX}}{10}} \times 10^{\frac{\mathrm{RX}}{10}} \times 10^{\frac{\mathrm{AD}}{10}} \times 10^{-\alpha\frac{\mathrm{R}}{10}} \quad (1)$$

where $d_R$ denotes the receiver aperture diameter (m), $d_T$ is the transmitter aperture diameter (m), $\theta$ represents the beam divergence (mrad), $R$ is the propagation range (km), $\alpha$ is the atmospheric attenuation coefficient (dB/km), $TX$ and $RX$ denote the transmitter and receiver losses (dB), respectively, and AD represents additional losses (dB).

## 2.1. OFDM signal generation

In the proposed DM-DD-OFDM-VLC system, the input binary data is mapped onto 16-QAM symbols. For an OFDM system with $N$ subcarriers, the complex baseband time-domain signal $x(t)$ generated after the inverse fast Fourier transform (IFFT) can be expressed as:

$$x(t) = \frac{1}{\sqrt{N}} \sum_{k=0}^{N\text{-}1} X_k e^{j2\pi k \Delta f t} \quad (2)$$

where $X_k$ represents the complex data symbol modulated onto the $k$-th subcarrier and $\Delta f$ is the subcarrier spacing. To mitigate inter-symbol interference (ISI) caused by channel dispersion, a cyclic prefix is appended to each OFDM symbol. By distributing the input data over a large number of orthogonal subcarriers, the OFDM structure increases the effective symbol duration of each subchannel, thereby reducing sensitivity to delay spread, while the cyclic prefix acts as a guard interval to preserve orthogonality and suppress residual ISI. The use of 512 active subcarriers within a 1024-point OFDM frame lowers the symbol rate of each subcarrier and thereby reduces sensitivity to delay spread, while the 10-sample cyclic prefix acts as a guard interval that suppresses residual ISI and preserves subcarrier orthogonality in the modeled LoS channel. In the present baseline LoS model, the

10-sample cyclic prefix is included as a guard interval to protect the OFDM symbol boundary under limited effective delay spread; it is not intended to establish robustness against strong dispersive or chirp-dominated channel conditions.

## 2.2. Channel and received signal

Assuming a short-to-medium range LoS channel where atmospheric turbulence is negligible, the channel is modeled primarily by its attenuation and geometric path loss. The received optical power $P_R$ is derived from the link budget as given in Equation (1). Consequently, the received electrical signal $y(t)$ after the PIN photodiode is given by:

$$y(t) = R[P_R \cdot x(t)] + n(t) \tag{3}$$

where R is the responsivity of the photodetector (1 A/W) and $n(t)$ encompasses the Additive White Gaussian Noise (AWGN), primarily dominated by thermal and shot noise at the receiver. It should be noted that the 500 m propagation analysis is based on a point-to-point LoS optical link-budget model dominated by geometric loss and attenuation; ambient background light and receiver field-of-view effects were not explicitly included in the present simulations and are left for future work.

At the receiver, the detected electrical signal is impaired by additive noise that is modeled through the dominant shot-noise and thermal-noise contributions associated with the photodetection and front-end circuitry. Accordingly, the total receiver-noise variance can be written as:

$$\sigma_n^2 = \sigma_{\text{shot}}^2 + \sigma_{\text{thermal}}^2. \tag{4}$$

The shot-noise variance is commonly expressed as:

$$\sigma_{\text{shot}}^2 = 2q\left(I_p + I_d\right)B \tag{5}$$

where (q) is the electron charge, ($I_p$) is the photocurrent generated by the received optical signal, ($I_d$) is the photodiode dark current, and (B) is the receiver electrical bandwidth. The thermal-noise variance can be represented as:

$$\sigma_{\text{thermal}}^2 = \frac{4kTB}{R_L}. \tag{6}$$

where ($k$) is Boltzmann's constant, (T) is the absolute temperature, and ($R_L$) is the equivalent load resistance of the receiver front end. Therefore, the AWGN term used in the BER/EVM analysis should be understood as an effective Gaussian representation of these dominant receiver-noise sources. In this expression, the additive noise term represents the equivalent Gaussian noise at the photodetector output, whose dominant components are the signal-dependent shot noise and the receiver thermal noise described above.

## 2.3. Performance metrics (EVM and BER)

To quantify the fidelity of the demodulated 16-QAM symbols, the EVM is calculated. EVM measures the variance between the ideal constellation points and the actual received symbols in the I-Q plane:

$$EVM_{RMS} = \sqrt{\frac{\frac{1}{K}\sum_{i=1}^{K}\left|S_{rx,i} - S_{tx,i}\right|^2}{P_{avg}}} \tag{7}$$

where $S_{rx,i}$ is the received symbol, $S_{tx,i}$ is the ideal transmitted symbol, $K$ is the number of evaluated symbols, and $P_{avg}$ is the average constellation power. The system's bit error rate (BER) is closely tied to the optical signal-to-noise ratio (OSNR). For an $M$-QAM modulated OFDM signal operating over an AWGN-dominant channel, the theoretical BER, $P_b$, can be approximated using the complementary error function ($Q$-function):

$$P_b \approx \frac{4}{\log_2(M)}\left(1\text{-}\frac{1}{\sqrt{M}}\right)Q\left(\sqrt{\frac{3 \cdot SNR}{M-1}}\right) \tag{8}$$

In this study ($M = 16$), ensuring a sufficiently high OSNR directly dictates the probability of maintaining the target BER threshold of $10^{-3}$. These theoretical relationships guide the parameter selection in the subsequent simulation framework.

The selection of 16-QAM in the proposed DM-DD-OFDM-VLC system reflects a compromise between spectral efficiency and error robustness. Since 16-QAM conveys 4 bits per symbol, it enables the system to achieve a high data rate of 15 Gbps while maintaining a moderate symbol rate of 3.75 Gsym/s. However, compared with lower-order modulation formats, the denser constellation of 16-QAM is more sensitive to noise and distortion, which increases the BER under insufficient OSNR conditions. Therefore, reliable operation with 16-QAM requires a sufficiently high OSNR to preserve accurate symbol detection, making OSNR a key design parameter for the proposed architecture.

# 3. System Model and Simulation Results

The proposed DM-DD-OFDM-VLC system architecture is depicted in the block diagram in Figure 1. System design, performance simulation, and data visualization were conducted using the OptiSystem software environment. As illustrated, the optical OFDM communication framework is categorized into three primary functional stages: the OFDM transmitter, the FSO channel, and the OFDM receiver.

The proposed system operates at a bit rate of 15 Gbps, corresponding to a symbol rate of 3.75 Gsym/s for 16-QAM (see Table 1). Key waveform parameters include a 1024-point fast Fourier transform (FFT) (utilizing 512 subcarriers), a 10-point cyclic prefix, and 10 training symbols. Given the short-to-medium range of the LoS configuration, the impact of atmospheric turbulence and attenuation is considered minimal and is thus omitted from the primary link-budget analysis. The simulation parameters listed in Table 1 were selected based on prior OFDM/VLC literature, standard component settings in OptiSystem, and the design requirements of the proposed DM-DD-OFDM-VLC link; the corresponding references are cited throughout the text where these parameters are introduced [35].

The transmitted bits are mapped and converted into different symbols based on the 16-QAM modulation using QAM sequence generators. The 16-QAM symbols, which are originally positioned in the frequency field, undergo a transformation into the time field via an IFFT operation. This critical process leads to the creation of a baseband OFDM signal, as illustrated in Figure 2(a). Figure 2(b) shows the power spectrum of the OFDM signal, plotted as power in dBm versus frequency in GHz centered at 0 Hz. The spectrum shows two symmetric main lobes peaking around ±2 GHz with power levels near –20 to –60 dBm and sidelobes that decay to around –60 dBm at higher frequency offsets. The OFDM signal is then modulated to increase its frequency to 7.5 GHz, thus producing a bandpass OFDM signal using an

**Figure 1**
**Schematic representation of the proposed DM-DD-OFDM-VLC architecture**

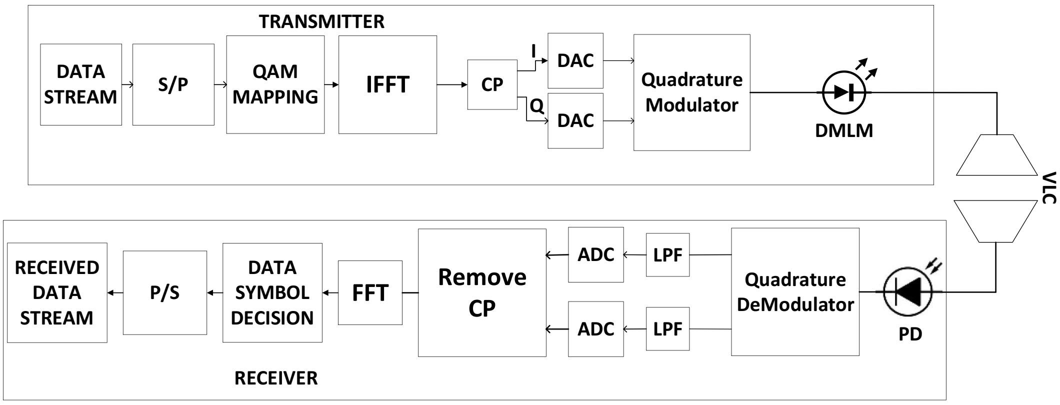


**Table 1**
**The primary parameters of the simulation**

| Type | Parameter name | Value |
|---|---|---|
| System parameters | Sequence length | 65536 bits |
| | Samples per bit | 4 |
| | Bit rate | 15 Gbps |
| | Number of samples | 262144 (16-QAM) |
| | Symbol rate | $3.75e^9$ Syms/s (16-QAM) |
| OFDM modulator, quadrature modulator, and demodulator | FFT points | 1024 |
| | Number of used subcarriers | 512 |
| | Cyclic prefix | 10 |
| | Number of training OFDM symbols | 10 |
| | Carrier frequency | 7.5 GHz |
| Directly modulated laser (DML) | Transmitted power ($P_T$) | 13.67 dBm |
| | Operating wavelength | 550 nm |
| | Linewidth | 10 MHz |
| | Maximum current | 300 mA |
| VLC channel | Main range | 500 m |
| | Attenuation (due to channel losses) | 2.5 dB/m |
| | Transmitter aperture diameter | 5 cm |
| | Beam divergence | 2 mrad |
| | Receiver aperture diameter | 20 cm |
| PIN photodiode | Dark current | 10 nA |
| | Responsivity type | Constant (1 A/W) |

electrical quadrature modulator at the transmitter, as illustrated in Figure 2(c). The electrical OFDM signal is modulated and transformed to an optical signal using a DML, which operates at a frequency of 550 nm and does not require a separate optical modulator such as a Mach–Zehnder modulator (MZM). It should be noted that the proposed transmitter is a directly modulated laser (DML) rather than a conventional phosphor LED; therefore, the severe LED nonlinearity and narrow modulation bandwidth commonly reported in indoor VLC systems are largely avoided in the present architecture. The system utilizes a DML, which is known to exhibit frequency chirp—a phenomenon where the laser's instantaneous frequency shifts with changes in injection current. However, for the short-to-medium range LoS links analyzed in this study, the impact of chirp-induced dispersion is considered negligible. By selecting a narrow laser linewidth of 10 MHz, the spectral broadening remains constrained, ensuring that the signal integrity is maintained over the atmospheric path without significant pulse distortion. The optical OFDM signal is shown in Figure 2(d). The optical OFDM signal was effectively sent over a 500 m VLC link. The transmitting antenna featured a diameter of 5 centimeters, while the receiver antenna boasted a larger diameter of 20 centimeters, enhancing its ability to capture the incoming light. With a beam divergence of 2 milliradians, the signal maintained a focused path, allowing for efficient transmission despite environmental challenges. The spectrum of the optical OFDM signal, after transmission through the VLC link,

**Figure 2**

**The spectrum of transmitted OFDM signal at different stages. Insets: (a) the frequency spectrum of transmitted baseband modulated QAM signal, (b) the frequency spectrum of transmitted OFDM signal after OFDM modulator, (c) the frequency spectrum of the transmitted and modulated bandpass OFDM signal, (d) the spectra of transmitted optical OFDM signal before VLC link, (e) the spectrum of the optical OFDM signal received after passing through the VLC link, (f) the frequency spectrum of received electrical bandpass OFDM signal, (g) the received electrical baseband OFDM signal, and (h) the received constellation diagram of 16-QAM signal**

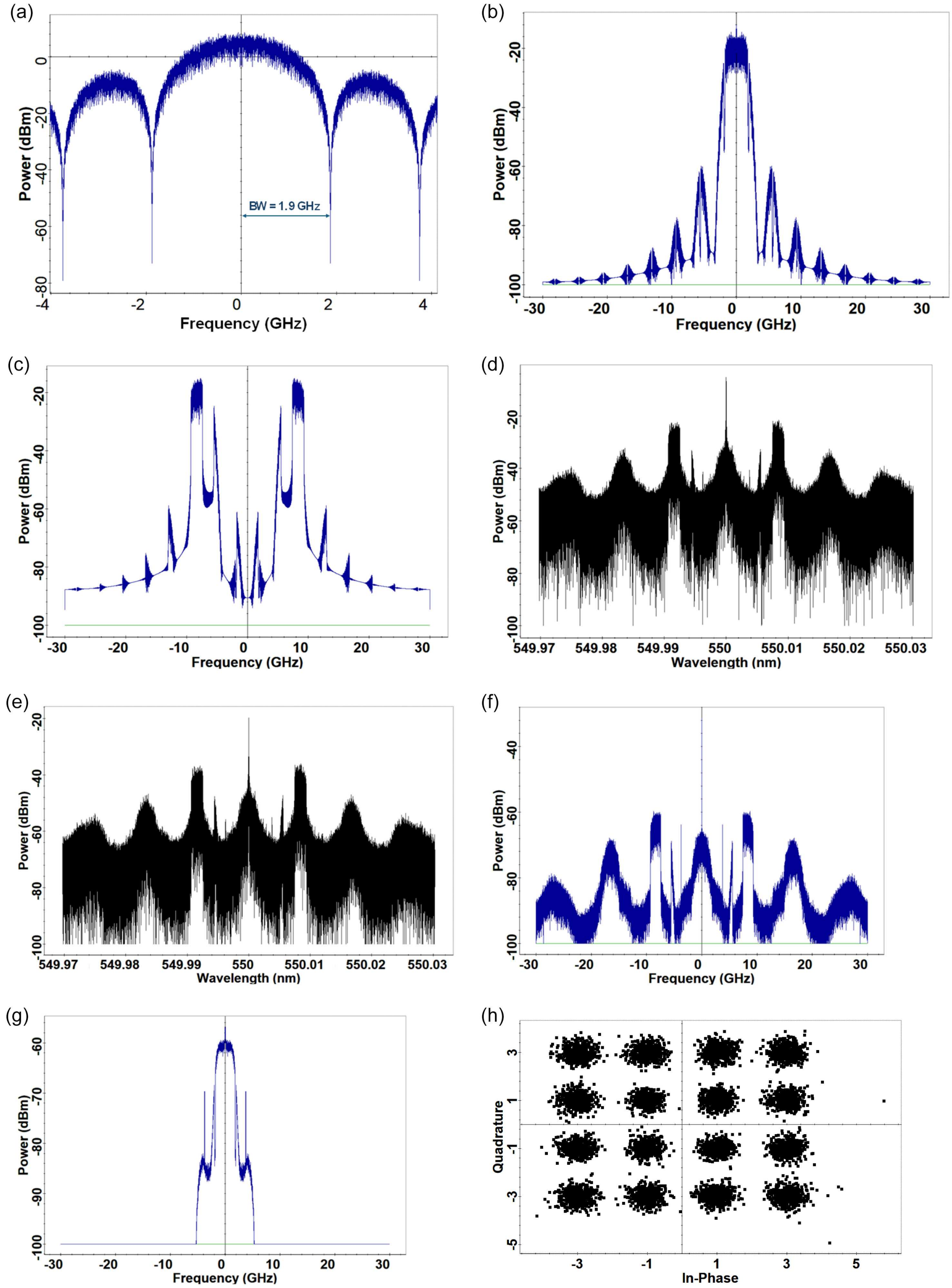

is illustrated in Figure 2(e). Figure 2(e) clearly shows the several wavelength values and their powers in dBm, highlighting how the VLC link affects the signal's characteristics during propagation. The PIN photodiode is utilized to convert the received optical OFDM signal into an electrical bandpass OFDM signal, as illustrated in Figure 2(f). A key parameter of the PIN photodiode is its responsivity, which is typically 1 A/W. Figure 2(f) shows that the power of the electrical bandpass OFDM signal for the 16-QAM scheme decreases with increasing frequency (from 0 to 20 GHz) due to greater attenuation and path loss at higher frequencies. A quadrature demodulator is utilized to demodulate received electrical bandpass OFDM signals, transforming them from high to low frequency and retrieving I-Q signals. The I-Q demodulated signal is subsequently processed through a low-pass filter, as illustrated in Figure 2(g). The main frequency of the demodulator is 7.5 GHz, while the cutoff frequency for the low-pass filter is 4.5 GHz (16-QAM). The OFDM demodulator is responsible for converting the demodulated signal into many orthogonal subcarriers. The QAM sequence decoder then decodes the demodulated OFDM signal into a binary format. Figure 2(h) illustrates the electrical diagram of the received symbols for 16 QAM at a 500 m VLC range. As shown in Figure 2(h), the constellation diagram of all QAM symbols is clear, and these symbols were correctly recovered at the receiver for our proposed optical OFDM system.

To evaluate the proposed 16-QAM DM-DD-OFDM-VLC architecture, the system's performance was simulated over a 500-m LoS optical link. The primary metrics for evaluation were EVM, OSNR, and BER.

### 3.1. BER, maximum Q factor, and OSNR characteristics

The relationship between OSNR and BER dictates the operational boundaries of our amplifier-free architecture, as depicted in Figure 3. The results demonstrate a clear, nonlinear thresholding effect. To maintain a BER below the Forward Error Correction (FEC) limit of $10^{-3}$, the system requires a minimum OSNR of 32 dB. This OSNR requirement is directly related to the use of 16-QAM modulation. While 16-QAM improves spectral efficiency by carrying 4 bits per symbol and thereby supports the targeted 15 Gbps throughput, its denser constellation is inherently more vulnerable to noise than lower-order modulation schemes. As a result, the BER performance becomes highly sensitive to OSNR degradation, and reliable detection is only achieved in a sufficiently high-OSNR regime. The results therefore confirm that 16-QAM provides an effective balance between transmission capacity and error performance for the proposed low-cost DM-DD-OFDM-VLC architecture. When the OSNR drops below this threshold, the BER degrades exponentially. From a physical hardware perspective, without the presence of a pre-amplifier (which would typically artificially boost the signal prior to detection), the signal at the lower OSNR bounds becomes fundamentally overwhelmed by the receiver's intrinsic thermal noise and the shot noise generated by the photodetector current. The ability of the system to achieve the FEC limit without external optical amplification validates the efficiency of pairing DMLs with 16-QAM OFDM for this specific range.

Figure 4 illustrates the relationship between the maximum Q factor and the OSNR in decibels (dB). Our proposed system achieves high Q factors when the OSNR exceeds 20 dB, as shown in Figure 4. For example, at an OSNR of 20 dB, the maximum Q factor reaches 8. A higher Q factor indicates better system performance and results in a lower BER.

**Figure 4**
**Maximum Q factor as a function of OSNR for the proposed system**

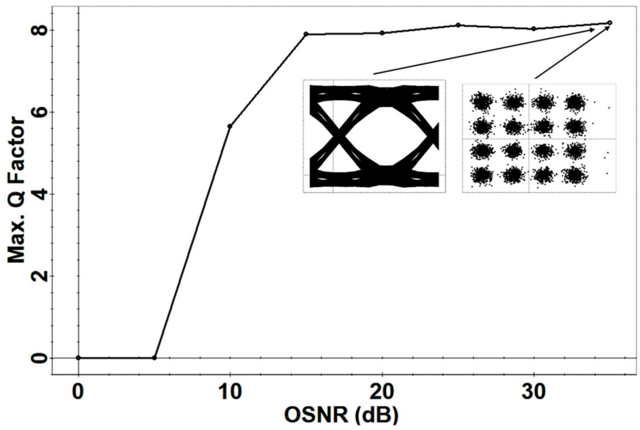


**Figure 3**
**BER as a function of OSNR for the proposed 16-QAM DM-DD-OFDM-VLC system**

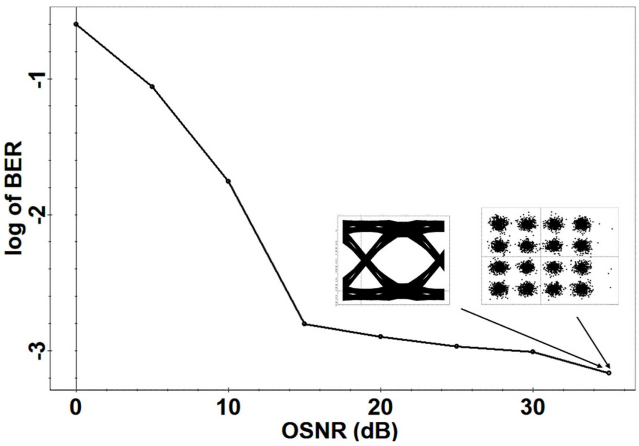


### 3.2. EVM and BER performance based on beam divergence limits

In VLC, the beam divergence angle is a fundamental optical parameter defining the angular spread of a transmitted laser beam as it propagates through the atmosphere. It is typically expressed in milliradians (mrad) and directly influences system performance by determining the footprint size of the beam at the receiver aperture. A narrow divergence angle produces a smaller spot size over long distances, increasing power density and maximizing received signal power, which is critical for maintaining high signal-to-noise ratios and achieving low BER performance. Figure 5 illustrates the correlation between beam divergence angle and BER performance. In our proposed system, it is essential for the beam divergence angle to remain within the range of 0 to 20 mrad to maintain a BER of $10^{-3}$. A larger beam divergence angle results in a decline in the system's performance, leading to an increased BER.

**Figure 5**
**BER performance as a function of beam divergence angle for the 500 m LoS link**

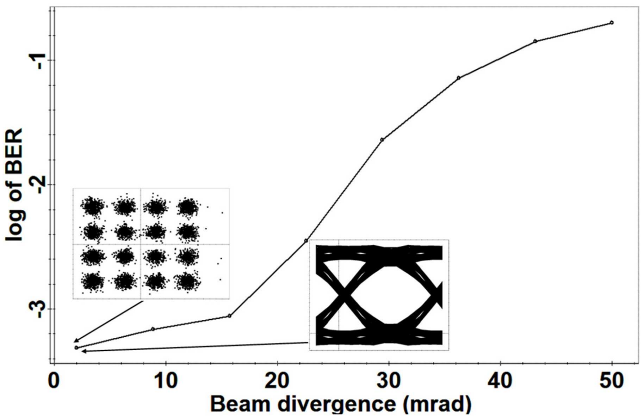


**Figure 6**
**EVM performance as a function of beam divergence angle**

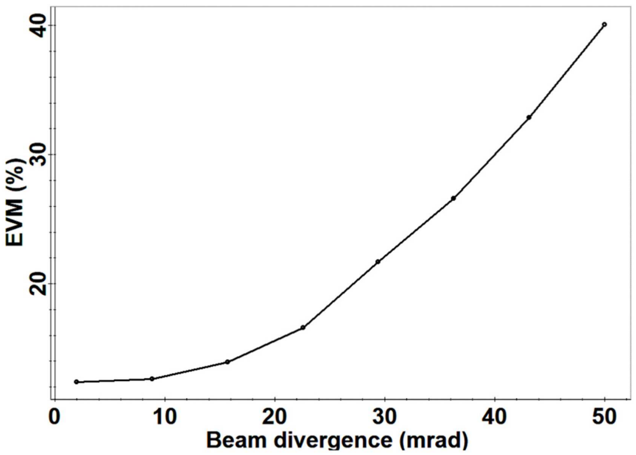


Figure 6 illustrates the received 16-QAM constellation diagrams and the corresponding EVM as a function of beam divergence angle. The system maintains a tightly clustered constellation and a low EVM at divergence angles below 15 mrad, indicating robust phase and amplitude fidelity of the directly modulated signal.

However, as the beam divergence exceeds 20 mrad, a sharp degradation in EVM is observed. Physically, this occurs due to two compounding factors. First, at a transmission distance of 500 m, an increased divergence angle exponentially expands the geometric footprint of the optical beam. This drastically reduces the spatial optical power density, meaning only a microscopic fraction of the transmitted photons successfully couple into the PIN photodiode's active area. Second, wider beam angles increase the spatial distribution of the light, heightening the probability of microscopic multipath reflections (even in nominally LoS environments). This introduces localized delay spreads that begin to interfere with the OFDM cyclic prefix, manifesting as ISI and scattering the received I-Q constellation points.

## 3.3. Power budget analysis of the proposed system

The link-budget calculation presented here corresponds to an idealized baseline model in which transmitter loss, receiver loss, and additional implementation losses are assumed to be 0 dB. Therefore, the agreement between theory and simulation validates the internal consistency of the adopted baseline model but does not represent a complete practical hardware loss budget. The received optical power at the PIN photodetector is determined by a link-budget analysis accounting for transmitted power, VLC channel parameters, and combined atmospheric and geometrical losses. These simulation results are benchmarked against theoretical derivations in Table 2. To characterize the power transfer function, a center wavelength of 550 nm was evaluated across varying propagation distances using a 16-QAM modulation scheme. From Table 1, the transmitted power ($P_T$) is 0.0232 $W$ = 13.67 dBm, the transmitter aperture diameter ($d_T$) is 0.05 m, the receiver aperture diameter ($d_R$) is 0.2 m, the beam divergence ($\theta$) is 2 mrad, atmospheric attenuation ($\alpha$) is 2.5 dB/m, and the transmitter loss (TX) and the receiver loss (RX) are 0 dB. Additional losses (AD) are 0 dB. For range ($R$) = 0.5 km, geometrical loss is $\frac{d_R^2}{(d_T+\theta R)^2}$ = 0.0363.

Now, $P_R = P_T \frac{d_R^2}{(d_T+\theta R)^2} 10^{\frac{TX}{10}} \times 10^{\frac{RX}{10}} \times 10^{\frac{AD}{10}} \times 10^{-\alpha\frac{R}{10}}$ $= 8.4132 \times 10^{-4}\, W = -0.7504\, dBm.$

Following this methodology, the received power was computed across a range of propagation distances, with the results summarized in Table 2.

Table 2 compares the received power values obtained through simulation and theoretical analysis. The negligible deviation between these datasets validates the analytical model. By applying the previously established equations across varying propagation distances, it is evident that the simulation results maintain high fidelity to theoretical predictions, as illustrated in Figure 7.

**Table 2**
**Comparative analysis of calculated and simulated values for the proposed system's received power across different coverage distances**

| Coverage range (km) | Theoretically calculated value of the received power (dBm) | Power received observed from the simulation setup (dBm) | Difference between the theoretical value and the simulation result |
|---|---|---|---|
| 0.5 | –0.7504 | –0.732 | 0.0184 |
| 0.875 | –5.4325 | –5.41 | 0.02257 |
| 1.25 | –8.45 | –8.45 | 0 |
| 1.625 | –10.69 | –10.72 | 0.024 |
| 2 | –12.47 | –12.48 | 0.01 |

**Figure 7**
**Received power comparison across propagation ranges**

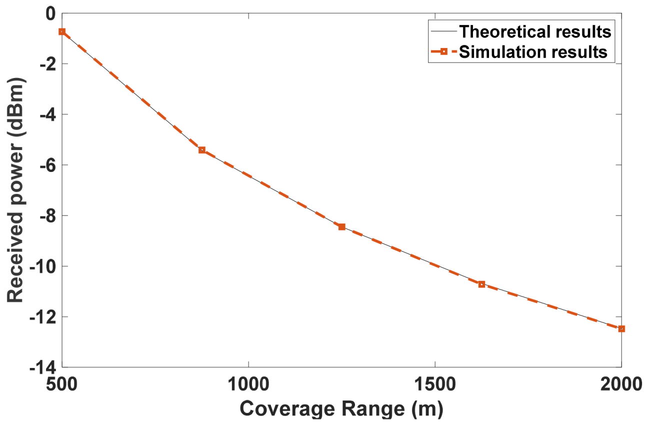


## 3.4. Comparative analysis and discussion

To contextualize the viability of the proposed system, it is necessary to compare these results against conventional VLC/FSO frameworks found in recent literature.

Traditional high-capacity optical links achieving upward of 10–20 Gbps over similar distances [38, 39] almost universally rely on external MZMs to avoid laser chirp, combined with optical amplifiers to overcome path loss. While those systems offer high signal fidelity, they suffer from high power consumption, large physical footprints, and significant implementation costs.

In contrast, our results demonstrate that a 15 Gbps throughput over 500 m is entirely feasible using a directly modulated architecture. By shifting the complexity from the optical hardware domain (eliminating external modulators/amplifiers) to the electrical digital signal processing domain (utilizing OFDM and 16-QAM), we achieve comparable data rates. The slight reduction in maximum achievable distance compared to amplified systems is a deliberate and acceptable trade-off for the substantial gains in cost-efficiency and system simplicity, making this architecture highly suitable for scalable, localized deployment.

By eliminating external optical modulators and Radio Frequency (RF)/electrical amplifiers, the proposed architecture reduces insertion loss, power consumption, and hardware complexity; however, this amplifier-free directly modulated configuration also reduces the available SNR margin, thereby making BER performance more sensitive to OSNR degradation and limiting the maximum practical transmission distance compared with externally modulated amplified links.

To better position the proposed system within the literature, Table 3 compares it with representative optical OFDM/VLC/OWC studies. Prior works have mainly focused either on ultra-high-capacity transmission or on advanced OFDM processing techniques, often with higher optical or implementation complexity. In contrast, the present work targets a directly

**Table 3**
**Comparison of the proposed system with representative optical OFDM/VLC/OWC studies**

| Reference | System/architecture | Main performance | Key distinction |
|---|---|---|---|
| [40] | Outdoor Li-Fi based on all-optical OFDM with optical IFFT processing | 1.2 Tbps over 1–100 km, with reported BER $\approx 1 \times 10^{-12}$ under modeled conditions | Very high-capacity architecture, but based on much higher optical complexity than the proposed directly modulated system |
| [38] | Outdoor Li-Fi using AO-OFDM under atmospheric turbulence and weather conditions | 640 Gbps over about 10 km, with BER $\approx 6 \times 10^{-4}$ in the reported scenario | Focuses on high-capacity outdoor performance under atmospheric impairments, rather than low-complexity implementation |
| [41] | Comparative study of multiple optical OFDM-VLC variants with Peak to Average Power Ratio (PAPR)-reduction analysis | Evaluates BER and PAPR across OFDM variants rather than one fixed end-to-end link | Useful as an algorithmic OFDM benchmark, but not focused on a simplified directly modulated hardware architecture |
| [35] | Low-cost DM-DD-OFDM-OWC architecture without external optical modulation at the transmitter | 15 Gbps; up to 200 km for higher-order formats with BER $\approx 10^{-3}$ in the reported OWC scenario | Closely related directly modulated concept, but developed for a different OWC/inter-satellite scenario than the present 500 m visible optical link |
| This work | DM-DD-OFDM-VLC link using a directly modulated laser with no external optical modulator and no transmission-line amplifier | 15 Gbps over 500 m LoS using 16-QAM, with BER $\leq 10^{-3}$ for OSNR $\approx$ 32 dB or higher | Emphasizes a compact, low-complexity, and energy-efficient architecture for short-to-medium-range visible optical wireless links |

modulated DM-DD-OFDM-VLC link that emphasizes a practical balance between transmission performance, hardware simplicity, and energy efficiency.

## 4. Conclusion

This paper investigated the performance of a directly modulated DM-DD-OFDM-VLC system intended for high-speed transmission with reduced hardware complexity. By employing 16-QAM modulation, a 1024-point FFT with 512 active subcarriers, and a DML source, the proposed system achieved a data rate of 15 Gbps over a 500 m LoS optical link without requiring external optical modulators or transmission-line amplifiers. The obtained results demonstrate that the proposed architecture can provide reliable communication under appropriate operating conditions while maintaining a simpler and more energy-efficient transmitter structure. The performance analysis showed that BER remains at or below the FEC threshold of $10^{-3}$ when the OSNR is approximately 32 dB or higher, indicating that the amplifier-free architecture requires a sufficiently strong signal quality margin for stable operation. The beam divergence analysis further revealed that the quality of the received signal strongly depends on optical beam confinement, since increasing divergence reduces the received power density and leads to EVM and BER degradation. In addition, the close agreement between theoretical and simulated received power values confirmed the validity of the adopted link-budget model. It should be noted that the present study does not include Non-Line-of-Sight (NLoS) propagation, weather-induced attenuation, mobility, or ambient background light, and therefore, the reported results should be interpreted as a baseline LoS performance assessment rather than a full outdoor deployment evaluation. Overall, the study confirms that the proposed directly modulated OFDM approach offers a practical trade-off between transmission performance, cost, hardware simplicity, and energy efficiency, making it suitable for short-to-medium-range localized visible optical wireless links. Future work will focus on experimental validation and on extending the analysis to more realistic channel conditions, including ambient light noise, receiver field-of-view effects, and non-LoS operation.

## Acknowledgment

This publication was supported by the Scientific Research Projects Coordination Unit of Istanbul Yeni Yuzyil University.

## Ethical Statement

This study does not contain any studies with human or animal subjects performed by the author.

## Conflicts of Interest

The author declares that he has no conflicts of interest to this work.

## Data Availability Statement

Data sharing is not applicable to this article as no new data were created or analyzed in this study.

## Author Contribution Statement

**Mahmoud Alhalabi:** Conceptualization, Methodology, Software, Validation, Formal analysis, Investigation, Resources, Data curation, Writing – original draft, Writing – review & editing, Visualization, Project administration.

## References

[1] Hou, Y., Wang, Z., Li, Z., Hu, J., Ma, C., Wang, X., . . . , & Shen, C. (2024). Laser-based mobile visible light communication system. *Sensors*, *24*(10), 3086. https://doi.org/10.3390/s24103086

[2] Al-Sammak, K. A., Al-Gburi, S. H., Marghescu, I., Drăgulinescu, A. M. C., Marghescu, C., Martian, A., . . . , & Al-Sammak, N. A. H. (2025). Optimizing LoRaWAN gateway placement in urban environments: A Hybrid PSO-DE algorithm validated via HTZ simulations. *Technologies*, *13*(6), 256. https://doi.org/10.3390/technologies13060256

[3] Pennanen, H., Hänninen, T., Tervo, O., Tölli, A., & Latva-Aho, M. (2024). 6G: The intelligent network of everything. *IEEE Access*, *13*, 1319–1421. https://doi.org/10.1109/ACCESS.2024.3521579

[4] Kharbouche, A., Madini, Z., Zouine, Y., & El-Haryqy, N. (2023). Signal demodulation with Deep Learning Methods for visible light communication. In *2023 9th International Conference on Optimization and Applications*, 1–5. https://doi.org/10.1109/ICOA58279.2023.10308822

[5] Kharbouche, A., Madini, Z., & Zouine, Y. (2021). Analysis of realistic DS-OCDMA/VLC for V2X communication using OptiSystem. In *2021 7th International Conference on Optimization and Applications*, 1–5. https://doi.org/10.1109/ICOA51614.2021.9442666

[6] Al Hasnawi, R., & Marghescu, I. (2024). A survey of vehicular VLC methodologies. *Sensors*, *24*(2), 598. https://doi.org/10.3390/s24020598

[7] Aghaei, F., Eldeeb, H. B., Bariah, L., Muhaidat, S., & Uysal, M. (2023). Comparative characterization of indoor VLC and mmw communications via ray tracing simulations. *IEEE Access*, *11*, 90345–90357. https://doi.org/10.1109/ACCESS.2023.3307186

[8] Waheed, A., Genoves Guzman, B., Mohammady, S., & Brandt-Pearce, M. (2026). A cross-layer framework integrating RF and OWC with dynamic modulation scheme selection for 6G networks. *Sensors*, *26*(3), 926. https://doi.org/10.3390/s26030926

[9] Sikder, P., Rahman, M. T., & Bakibillah, A. S. M. (2025). Advancements and challenges of visible light communication in intelligent transportation systems: A comprehensive review. *Photonics*, *12*(3), 225. https://doi.org/10.3390/photonics12030225

[10] Gupta, S., Roy, D., Bose, S., Dixit, V., & Kumar, A. (2024). Illuminating the future: A comprehensive review of visible light communication applications. *Optics & Laser Technology*, *177*, 111182. https://doi.org/10.1016/j.optlastec.2024.111182

[11] Han, X., Wang, W., Li, P., Li, G., Nie, W., Xie, Z., . . . , & Xie, X. (2025). Demonstration of anti-diffracting optical pin-like beam enabled 5Gbit/s OFDM underwater wireless optical communication system. *Optics Communications*, *579*, 131582. https://doi.org/10.1016/j.optcom.2025.131582

[12] Al-Hamiri, M. G., & Abd, H. J. (2024). Enhancing the performance of LiFi communication with OSTBC, QAM, and

OFDM: High-capacity, low-complexity transceiver design. *Results in Optics*, *16*, 100675. https://doi.org/10.1016/j.rio.2024.100675

[13] El-Nahal, F. I., & Abualoff, N. M. (2020). Coherent optical communication systems based on orthogonal frequency division multiplexing. *Optoelectronics Letters*, *16*(4), 303–305. https://doi.org/10.1007/s11801-020-9166-2

[14] Camporez, H., Costa, W., Pontes, M., Segatto, M., Rocha, H., Silva, J., . . . , & Freund, R. (2023). Increasing the reach of visible light communication links through constant-envelope OFDM signals. *Optics Communications*, *530*, 129179. https://doi.org/10.1016/j.optcom.2022.129179

[15] Wen, H., Chen, H., Chen, Q., Luo, K., Chen, M., & Liu, F. (2023). Performance enhanced dual-mode index modulation OFDM with OCT precoding in VLC systems. *Optics Communications*, *530*, 129191. https://doi.org/10.1016/j.optcom.2022.129191

[16] Mallaiah, R., Miriyala, G., K.S, A., & Mani, V. V. (2024). A low-complex OFDM based DCO-OTFS modulation for VLC systems. *Physical Communication*, *66*, 102471. https://doi.org/10.1016/j.phycom.2024.102471

[17] Zenhom, Y. A., Hamad, E. K. I., Elkarim, M. A., & Elnabawy, M. M. (2025). Alleviating high PAPR and noise issues for optimized performance in ACO-OFDM-Based VLC systems. *Optics & Laser Technology*, *188*, 112950. https://doi.org/10.1016/j.optlastec.2025.112950

[18] Dahri, F. A., Ali, S., & Jawaid, M. M. (2018). A review of modulation schemes for visible light communication. *International Journal of Computer Science and Network Security*, *18*(2), 117–125.

[19] Loureiro, P. A., Guiomar, F. P., & Monteiro, P. P. (2023). Visible light communications: A survey on recent high-capacity demonstrations and digital modulation techniques. *Photonics*, *10*(9), 993. https://doi.org/10.3390/photonics10090993

[20] Vappangi, S., Mani, V. V., & Sellathurai, M. (2021). *Visible light communication: A comprehensive theory and applications with MATLAB®*. USA: CRC Press. https://doi.org/10.1201/9781003191537

[21] Othman, N., Che Beson, M. R., Aljunid, S. A., & Endut, R. (2024). A review: Outdoor visible light communication on modulation and receiver denoising scheme. *AIP Conference Proceedings*, *2898*(1), 030038. https://doi.org/10.1063/5.0195503

[22] Zhang, X., Babar, Z., Petropoulos, P., Haas, H., & Hanzo, L. (2021). The evolution of optical OFDM. *IEEE Communications Surveys & Tutorials*, *23*(3), 1430–1457. https://doi.org/10.1109/COMST.2021.3065907

[23] Che, M. (2025). Software-defined visible light communication for Internet of Things: A low-complexity approach. *Telecom*, *6*(2), 31. https://doi.org/10.3390/telecom6020031

[24] Jativa, P. P., Azurdia-Meza, C. A., Canizares, M. R., Zabala-Blanco, D., & Montejo-Sanchez, S. (2020). Performance analysis of OFDM-based VLC schemes in NLOS channels. In *2020 South American Colloquium on Visible Light Communications* (pp. 1–6). https://doi.org/10.1109/SACVLC50805.2020.9129862

[25] Sun, Y., Yang, F., & Gao, J. (2017). Comparison of hybrid optical modulation schemes for visible light communication. *IEEE Photonics Journal*, *9*(3), 1–13. https://doi.org/10.1109/JPHOT.2017.2705040

[26] Wu, Y., Li, Y., & Li, B. (2025). Low-PAPR ASE-DMT using constellation extension for optical wireless communications. *Sensors*, *25*(16), 5109. https://doi.org/10.3390/s25165109

[27] Vijayakumari, K., & Anusudha, K. (2024). A comprehensive study on the advances and challenges in visible light communication technologies. In *2024 Third International Conference on Smart Technologies and Systems for Next Generation Computing (ICSTSN)*, 1–6. https://doi.org/10.1109/ICSTSN61422.2024.10671207

[28] Lian, J., Vatansever, Z., Noshad, M., & Brandt-Pearce, M. (2019). Indoor visible light communications, networking, and applications. *Journal of Physics: Photonics*, *1*(1), 012001. https://doi.org/10.1088/2515-7647/aaf74a

[29] Rahman, A. B. M. M., Li, T., & Wang, Y. (2020). Recent advances in indoor localization via visible lights: A survey. *Sensors*, *20*(5), 1382. https://doi.org/10.3390/s20051382

[30] Sliti, M., Mrabet, M., Garai, M., & Ammar, L. B. (2024). A survey on machine learning algorithm applications in visible light communication systems. *Optical and Quantum Electronics*, *56*(8), 1351. https://doi.org/10.1007/s11082-024-06862-1

[31] Arafa, N. A., El-Att, S. M. A., Eldeeb, H. B., & Arafa, M. S. (2024). Deep learning-based automatic modulation format identification for I2V visible light communication. In *2024 41st National Radio Science Conference*, 191–199. https://doi.org/10.1109/NRSC61581.2024.10510466

[32] Eldeeb, H. B., Qaraqe, M., Muhaidat, S., & Ghrayeb, A. (2024). Reconfigurable intelligent surfaces-assisted I2V-visible light communication. In *2024 IEEE International Mediterranean Conference on Communications and Networking*, 465–470. https://doi.org/10.1109/MeditCom61057.2024.10621213

[33] Alhalabi, M., Taşpınar, N., & Wadi, M. (2025). PAPR reduction using discrete forest optimization algorithm based on SLM technique in intensity modulated direct detection optical OFDM communication systems. *International Journal of Communication Systems*, *38*(10), e70126. https://doi.org/10.1002/dac.70126

[34] Alhalabi, M., Taşpınar, N., & Sönmezocak, T. (2026). A novel hybrid whale optimization algorithm-based SLM (HWOA-SLM) for PAPR reduction in optical IM/DD OFDM systems. *Applied Sciences*, *16*(5), 2349. https://doi.org/10.3390/app16052349

[35] Alhalabi, M., Taşpınar, N., Wadi, M., & Salemdeeb, M. (2026). Performance analysis of a low-cost directly modulated OFDM-based optical wireless communication systems. *Wireless Personal Communications*, *146*(3), 1415–1441. https://doi.org/10.1007/s11277-026-11927-3

[36] El-Nahal, F., Xu, T., AlQahtani, D., & Leeson, M. (2023). A bidirectional WDM-PON free space optical (FSO) system for fronthaul 5 G C-RAN networks. *IEEE Photonics Journal*, *15*(1), 1–10. https://doi.org/10.1109/JPHOT.2022.3232081

[37] El-Nahal, F., Xu, T., AlQahtani, D., & Leeson, M. (2022). A bidirectional wavelength division multiplexed (WDM) free space optical communication (FSO) system for deployment in data center networks(DCNs). *Sensors*, *22*(24), 9703. https://doi.org/10.3390/s22249703

[38] Mohsin, M. J., & Murdas, I. A. (2023). Performance analysis of an outdoor Li-Fi system-based AO-OFDM architecture under different FSO turbulence and weather conditions. *Optik*, *273*, 170427. https://doi.org/10.1016/j.ijleo.2022.170427

[39] Oria Oria, A. C., Becerra, J. A., Madero-Ayora, M. J., Baena Lecuyer, V., & Crespo-Cadenas, C. (2025). Symbol constellation predistortion for DCO-OFDM visible light communications system linearization. *Digital Signal Processing*, *165*, 105310. https://doi.org/10.1016/j.dsp.2025.105310

[40] Mohsin, M. J., & Murdas, I. A. (2022). Design an outdoor Light Fidelity (Li-Fi) system based on all-optical OFDM architecture. *International Journal of Intelligent Engineering and Systems*, *15*(3), 193–204. https://doi.org/10.22266/ijies2022.0630.16

[41] Zenhom, Y. A., Hamad, E. K. I., Alghassab, M., & Elnabawy, M. M. (2024). Optical-OFDM VLC system: Peak-to-average power ratio enhancement and performance evaluation. *Sensors*, *24*(10), 2965. https://doi.org/10.3390/s24102965

**How to Cite:** Alhalabi, M. (2026). Performance Analysis of a 16-QAM Directly Modulated OFDM Visible Optical Wireless Link Without External Modulators. *Journal of Optics and Photonics Research*. https://doi.org/10.47852/bonviewJOPR62029416